



ISSN 0975-413X  
CODEN (USA): PCHHAX

Der Pharma Chemica, 2016, 8(4):85-95  
(<http://derpharmachemica.com/archive.html>)

## Synthesis of novel pyrido[2,3-b]pyrazine derivative evaluated theoretically and electrochemically as a corrosion inhibitor for mild steel in 1M HCl solutions

M. Y. Hjouji<sup>1</sup>, M. Djedid<sup>4</sup>, H. Elmsellem<sup>2</sup>, Y. Kandri Rodi<sup>1\*</sup>, M. Benalia<sup>4</sup>, H. Steli<sup>5</sup>,  
Y. Ouzidan<sup>1</sup>, F. Ouazzani Chahdi<sup>1</sup>, E. M. Essassi<sup>3</sup> and B. Hammouti<sup>2</sup>

<sup>1</sup>Laboratory of Applied Organic Chemistry, Faculty of Science and Technology, Sidi Mohammed Ben Abdellah University, Fez, Morocco

<sup>2</sup>Laboratoire de chimie analytique appliquée, matériaux et environnement (LC2AME), Faculté des Sciences, B.P. 717, 60000 Oujda, Morocco

<sup>3</sup>Laboratoire de Chimie Organique Hétérocyclique, URAC 21, Pôle de Compétences Pharmacochimie, Mohammed V University, Av. Ibn Battouta, BP 1014 Rabat, Morocco

<sup>4</sup>Laboratory of Process Engineering, Department Process Engineering, Laghouat University, P.O Box 37G, Route de Ghardaïa, 03000, Laghouat, Algeria

<sup>5</sup>Laboratoire Mécanique & Energétique, Faculté des Sciences, Université Mohammed Premier, Oujda, Maroc

### ABSTRACT

pyrido[2,3-b]pyrazine (P1) was synthesized and its inhibiting action on the corrosion of mild steel in 1 M hydrochloric acid was examined by different corrosion methods, such as weight loss, potentiodynamic polarization and electrochemical impedance spectroscopy (EIS). The experimental results suggest that this compound is an efficient corrosion inhibitor and the inhibition efficiency increases with the increase in inhibitor concentration. Adsorption of this compound on mild steel surface obeys Langmuir's isotherm. Correlation between quantum chemical calculations and inhibition efficiency of the investigated compound is discussed using the Density Functional Theory method (DFT).

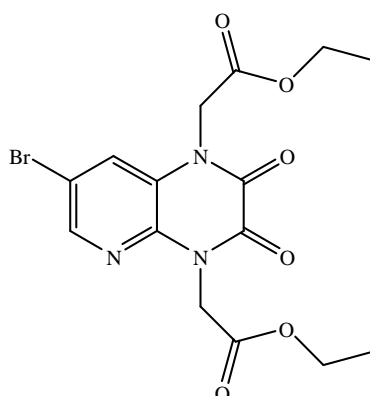
**Keywords:** corrosion inhibition, pyrido[2,3-b]pyrazine, weight loss, polarization, adsorption, DFT.

### INTRODUCTION

Pyrido[2,3-b]pyrazine (5-azaquinoxaline) derivatives is a structural analogue of pteridine and quinoxaline. They constitute a very important nitrogen-containing heterocycles, widely used for their pharmacological, therapeutic and others properties [1-3]. Studies have shown that such compounds are widely involved in several fields, as anti-malarial [4], anti-cancer [5], antibacterial [6] and antiallergic properties [7]. pyrido[2,3-b]pyrazine derivatives continue to attract considerable attention because of their strong inhibitory activities of phosphodiesterase IV (PDE IV) and the production of tumor necrosis factor (TNF) [8]. Several classes of organic compounds like pyridopyrazine derivative are broadly used as corrosion inhibitors for metals in acid environments, since they own the nitrogen and oxygen atoms which can easily be protonated to exhibit good inhibitory action on the corrosion of metals [9-13].

In this work, we have chosen to synthesis a new compound named [7-bromo-1,4-bis(acétate d'éthyl-yl)pyrido[2,3-b]pyrazine-2,3(1H,4H)-dione]:(P1) by the N-alkylation of 7-bromopyrido [2,3-b] pyrazine-2,3 (1H, 4H) -dione (2) with ethyl 2-bromoacetate under the conditions of the phase transfer catalysis solid-liquid [14] allows to isolate the

expected compound (P1) and evaluate the corrosion inhibition efficiency of mild steel in 1 M hydrochloric acid solution.

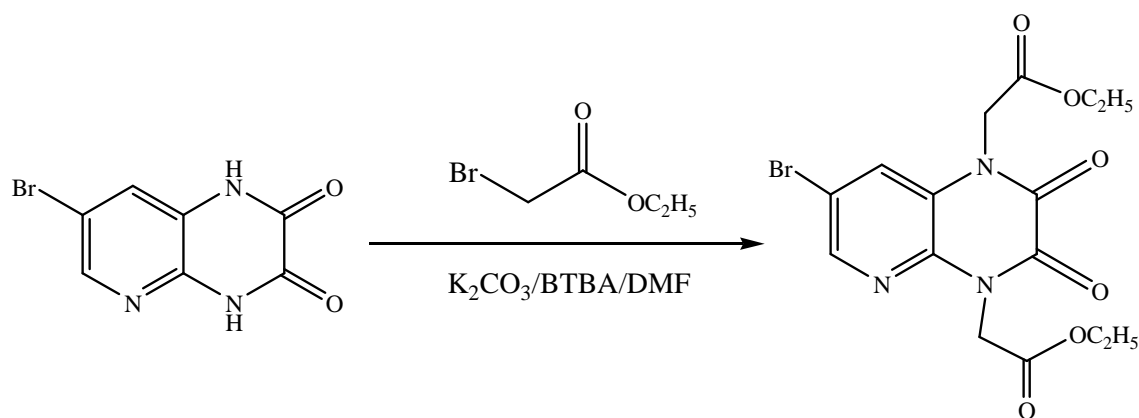


Scheme 1: 7-bromo-1,4-bis(acétate d'éthyl-yl)pyrido[2,3-b]pyrazine-2,3(1H,4H)-dione: (P1)

## MATERIALS AND METHODS

### 2.1. Synthesis of inhibitors

In a flask equipped with a magnetic stirrer, we put 7-bromopyrido [2,3-b] pyrazine-2,3 (1H, 4H) -dione (**2**) (1 mmol, 0.25g), 20 ml of DMF, potassium carbonate  $K_2CO_3$  (2.1 mmol, 0.29g), tétra-n-butylammonium bromide (TBAB) (0.2 mmol, 0.064g) with stirring for 5 min; Then, we added dropwise 0.18 ml of ethyl 2-bromoacetate (2 mmol). The reaction is brought at room temperature for 6 hours. After removal of salts by filtration, the DMF is evaporated under reduced pressure and the residue obtained is dissolved in dichloromethane. The rest of the salts are removed by washing the organic phase three times with distilled water. Concentrated to dryness, the compound desired is purified by flash column chromatography (on silica-gel with ethyl acetate: hexane, 1:1) to afford 7-bromo-1,4-bis(acétate d'éthyl-yl)pyrido[2,3-b] pyrazine-2,3(1H,4H)-dione (**P1**) (R= 85%) as a yellow solid. (M.p 465-466 K) **Scheme 2:**



Scheme 2: Synthesis of 7-bromo-1,4-bis(acétate d'éthyl-yl)pyrido[2,3-b]pyrazine-2,3(1H,4H)-dione (P1)

**Compound (P1):** Yield = 90%; M.p 465-466 K;  $^{1}H$  RMN  $\delta$ ppm: 8.274 (d, 1H, H pyr); 7.408 (d, 1H, H pyr); 5.136, 4.924 (s, 4H,  $CH_2$ -N); 4.215-4.349 (2q, 4H, O- $CH_2$ ); 1.305, 1.329 (2t, 6H, 2 - $CH_3$ ).  $^{13}C$  RMN  $\delta$ ppm: 166.93 (2 O-C=O); 166.02 (2 C=O); 143.39, 124.06 (-CH pyr); 137.26, 123.99, 114.92 (Cq); 62.57, 61.85 (N- $CH_2$ ); 44.13, 43.10 (2 O- $CH_2$ ); 14.08 (2  $CH_3$ ).

### 2.2. Solutions

The aggressive solutions of 1.0 M HCl were prepared by dilution of an analytical grade 37% HCl with double distilled water. The concentration range of inhibitor P4 employed was  $10^{-6}$ - $10^{-3}$  (mol/l).

### 2.3. Weight loss Method

Coupons were cut into  $1.5 \times 1.5 \times 0.05$  cm<sup>3</sup> dimensions having composition (0.09%P, 0.01 % Al, 0.38 % Si, 0.05 % Mn, 0.21 % C, 0.05 % S and Fe balance) used for weight loss measurements. Prior to all measurements, the exposed area was mechanically abraded with 180, 400, 800, 1000, 1200 grades of emery papers. The specimens are washed thoroughly with bidistilled water degreased and dried with ethanol. Gravimetric measurements are carried out in a

double walled glass cell equipped with a thermostated cooling condenser. The solution volume is 100 cm<sup>3</sup>. The immersion time for the weight loss is 6 h at (308±1) K. In order to get good reproducibility, experiments were carried out in duplicate. The average weight loss was obtained. The corrosion rate ( $v$ ) is calculated using the following equation:

$$v = W / S.t \quad (1)$$

Where  $W$  is the average weight loss,  $S$  the total area, and  $t$  is immersion time. With the corrosion rate calculated, the inhibition efficiency ( $E_w$ ) is determined as follows:

$$E_w \% = \frac{v_0 - v}{v_0} \times 100 \quad (2)$$

Where  $V_0$  and  $V$  are the values of corrosion rate without and with inhibitor, respectively.

#### 2.4. Polarization Measurements

The electrochemical study was carried out using a potentiostat PGZ100 piloted by Voltmaster soft-ware. This potentiostat is connected to a cell with three electrode thermostats with double wall. A saturated calomel electrode (SCE) and platinum electrode were used as reference and auxiliary electrodes, respectively. Anodic and cathodic potentiodynamic polarization curves were plotted at a polarization scan rate of 0.5mV/s. Before all experiments, the potential was stabilized at free potential during 30 min. The polarisation curves are obtained from -800 mV to -200 mV at 308 K. The solution test is there after de-aerated by bubbling nitrogen. Inhibition efficiency ( $E_p$ %) is defined as:

$$E_p \% = \frac{i_{cor(0)} - i_{cor(inh)}}{i_{cor(0)}} \times 100 \quad (3)$$

Where  $i_{cor(0)}$  and  $i_{cor(inh)}$  represent corrosion current density values without and with inhibitor, respectively.

#### 2.5. Impedance measurements

The electrochemical impedance spectroscopy (EIS) measurements are carried out with the electrochemical system, which included a digital potentiostat model Voltalab PGZ100 computer at  $E_{corr}$  after immersion in solution without bubbling. After the determination of steady-state current at a corrosion potential, sine wave voltage (10 mV) peak to peak, at frequencies between 100 kHz and 10 mHz are superimposed on the rest potential. Computer programs automatically controlled the measurements performed at rest potentials after 0.5 hour of exposure at 308 K. The impedance diagrams are given in the Nyquist representation.

Inhibition efficiency ( $E_R$ %) is estimated using the relation:

$$E_R \% = \frac{R_t(inh) - R_t(0)}{R_t(inh)} \times 100 \quad (4)$$

Where  $R_t(0)$  and  $R_t(inh)$  are the charge transfer resistance values in the absence and presence of inhibitor, respectively.

#### 2.6. Computational Chemistry

All the quantum chemical calculations have been carried out with Gaussian 09 programme package [15-16]. In our calculation we have used B3LYP, a hybrid functional of the DFT method, which consists of the Becke's three parameters; exact exchange functional B3 combined with the nonlocal gradient corrected correlation functional of Lee-Yang-Par (LYP) has been used along with 6-31G(dp) basis set. In the process of geometry optimisation for the fully relaxed method, convergence of all the calculations has been confirmed by the absence of imaginary frequencies. The aim of our calculation is to calculate the following quantum chemical indices: the energy of highest occupied molecular orbital ( $E_{HOMO}$ ), the energy of lowest unoccupied molecular orbital ( $E_{LUMO}$ ), energygap ( $\Delta E$ ), hardness ( $\eta$ ), softness ( $\sigma$ ), electrophilicity index ( $\omega$ ), the fraction of electrons transferred ( $\Delta N$ ) from inhibitor molecule to the metal surface, and energy change when both processes occur, namely, and correlate these with the experimental observations. The electronic populations as well as the Fukui indices and local nucleophilicities are computed using different populations analysis MPA (Mulliken population analysis) and NPA (natural population analysis) [17-19]. The cationic systems, needed in the calculation of nucleophilic Fukui indices, are taken in the same geometry as the neutral system. Our objective, in this study, is to investigate computationally inhibitory action

of quinoline derivative **P1** with chloridric acid in gas and in aqueous phase using B3LYP method with 6-31G(d,p) basis set.

### 2.6.1. Theory and computational details

Theoretical study of quinoline derivative with chloridric acid as corrosion inhibitors was done by using the Density Functional Theory (DFT) with the B3LYP [20] /6-31G(d,p) method implemented in Gaussian 09 program package.

In this study, some molecular properties were calculated such as the frontier molecular orbital (HOMO and LUMO) energies, energy gap ( $E_{\text{Gap}}$ ), charge distribution, electron affinity (A), ionization

Popular qualitative chemical concepts such as electronegativity [21, 22] ( $\chi$ ) and hardness [23] ( $\eta$ ) have been provided with rigorous definitions within the purview of conceptual density functional theory [24-26] (DFT). Electronegativity is the negative of chemical potential defined [27] as follows for an N-electron system with total energy E and external potential  $v(\vec{r})$

$$\chi = -\mu = -\left(\frac{\partial E}{\partial N}\right)_{v(r)} \quad (5)$$

$\mu$  is the Lagrange multiplier associated with the normalization constraint of DFT [28, 29].

Hardness ( $\eta$ ) is defined [30] as the corresponding second derivative,

$$\eta = -\left(\frac{\partial^2 E}{\partial N^2}\right)_{v(r)} = -\left(\frac{\partial \mu}{\partial N}\right)_{v(r)} \quad (6)$$

Using a finite difference method, working equations for the calculation of  $\chi$  and  $\eta$  may be given as [24]:

$$\chi = \frac{I+A}{2} \quad \text{or} \quad \chi = -\frac{E_{\text{HOMO}} + E_{\text{LUMO}}}{2} \quad (7)$$

$$\eta = \frac{I-A}{2} \quad \text{or} \quad \eta = -\frac{E_{\text{HOMO}} - E_{\text{LUMO}}}{2} \quad (8)$$

Where  $I = -E_{\text{HOMO}}$  and  $A = -E_{\text{LUMO}}$  are the ionization potential and electron affinity respectively.

Local quantities such as Fukui function  $f(r)$  defined the reactivity/selectivity of a specific site in a molecule. The Fukui function is defined as the first derivative of the electronic density  $q(r)$  of a system with respect to the number of electrons N at a constant external potential  $v(r)$  [31].

$$f(r) = \left[\frac{\partial \rho(r)}{\partial N}\right]_{v(r)} = \left[\frac{\delta \mu}{\delta v(r)}\right]_N \quad (9)$$

Using left and right derivatives with respect to the number of electrons, electrophilic and nucleophilic Fukui functions for a site k in a molecule can be defined [32].

$$f_k^+ = P_k(N+1) - P_k(N) \quad \text{for nucleophilic attack} \quad (10)$$

$$f_k^- = P_k(N) - P_k(N-1) \quad \text{for electrophilic attack} \quad (11)$$

$$f_k^+ = [P_k(N+1) - P_k(N-1)]/2 \quad \text{for radical attack} \quad (12)$$

Where,  $P_k(N)$ ,  $P_k(N+1)$  and  $P_k(N-1)$  are the natural populations for the atom k in the neutral, anionic and cationic species respectively.

The fraction of transferred electrons  $\Delta N$  was calculated according to Pearson theory [33]. This parameter evaluates the electronic flow in a reaction of two systems with different electronegativities, in particular case; a metallic surface (Fe) and an inhibitor molecule.  $\Delta N$  is given as follows:

$$\Delta N = \frac{\chi_{Fe} - \chi_{inh}}{2(\eta_{Fe} + \eta_{inh})} \quad (13)$$

where  $\chi_{Fe}$  and  $\chi_{inh}$  denote the absolute electronegativity of an iron atom (Fe) and the inhibitor molecule, respectively;  $\eta_{Fe}$  and  $\eta_{inh}$  denote the absolute hardness of Fe atom and the inhibitor molecule, respectively. In order to apply the eq. 8 in the present study, a theoretical value for the electronegativity of bulk iron was used  $\chi_{Fe} = 7$  eV and a global hardness of  $\eta_{Fe} = 0$ , by assuming that for a metallic bulk  $I = A$  because they are softer than the neutral metallic atoms [33].

The electrophilicity has been introduced by Parr et al. [34], is a descriptor of reactivity that allows a quantitative classification of the global electrophilic nature of a compound within a relative scale. They have proposed the  $\omega$  as a measure of energy lowering owing to maximal electron flow between donor and acceptor and  $\omega$  is defined as follows.

$$\omega = \frac{\chi^2}{2\eta} \quad (14)$$

The softness  $\sigma$  is defined as the inverse of the  $\eta$  [35]

$$\sigma = \frac{1}{\eta} \quad (15)$$

## RESULTS AND DISCUSSION

### 3.1. Gravimetric measurements

The effect of addition of P1 at different concentrations on the corrosion of Mild steel in 1M HCl solution was studied by weight loss at 6 h. Table 1 gathers the values deduced of  $W_{corr}$  and the inhibition efficiency ( $E_w\%$ ) determined.

Table 1 indicates clearly a decrease in the corrosion rate in the presence of P1. This effect is hugely marked at higher concentration of inhibitor P1. The inhibitive action is more explicit by  $E_w\%$  data which increases with inhibitor concentration to reach 93% for P1 at  $10^{-3}M$  to exhibit the best inhibitory action.

**Table 1. Corrosion parameters obtained from weight loss measurements for mild steel in 1 M HCl containing various concentrations of (P1) at 308 K**

Inhibitor	Concentration (M)	w (mg.cm <sup>-2</sup> .h <sup>-1</sup> )	E <sub>w</sub> (%)
1 M HCl	--	0.82	--
Inhibitor P1	10 <sup>-6</sup>	0.45	45
	10 <sup>-5</sup>	0.23	72
	10 <sup>-4</sup>	0.11	87
	10 <sup>-3</sup>	0.06	93

Adsorption isotherms are very important in determining the mechanism of organic electrochemical reactions. The most frequently used adsorption isotherms are Langmuir, Temkin and Frumkin. So several adsorption isotherms were tested for the description of adsorption behaviour of studied compound and it is found that adsorption of compound under study obeys the Langmuir adsorption isotherm (Figure 1). The experimental result is in good agreement with the Langmuir adsorption isotherm, which is represented by the following equation (eq. 16) [36]:

$$C/\theta = 1/K_{ads} + C \quad (16)$$

where  $\theta$  is the degree of surface coverage,  $K_{ads}$  is the equilibrium constant of the adsorption process and  $C_{inh}$  is the concentration of the inhibitor.

$K_{ads}$  is the equilibrium constant of the adsorption process and is related to the standard Gibbs energy of adsorption,  $\Delta G_{ads}$ , according to:

$$\Delta G_{ads} = -RT \ln(55.55 K_{ads}) \quad (17)$$

Where  $R$  is the universal gas constant and  $T$  is the absolute temperature. The value 55.55 in the above equation is the concentration of water in solution in mol/l. Thermodynamic parameters is important to study the inhibitive mechanism. The values of  $K_{ads}$ ,  $R^2$  and  $\Delta G_{ads}$  are calculated and are (out) given in Table 2. The relation between

$C_{inh}/\theta$  and  $C_{inh}$  is shown in Figure 1. These plots are linear with a slope equal to unity. This suggests that the adsorption of P1 on metal surface followed the Langmuir adsorption isotherm [37].

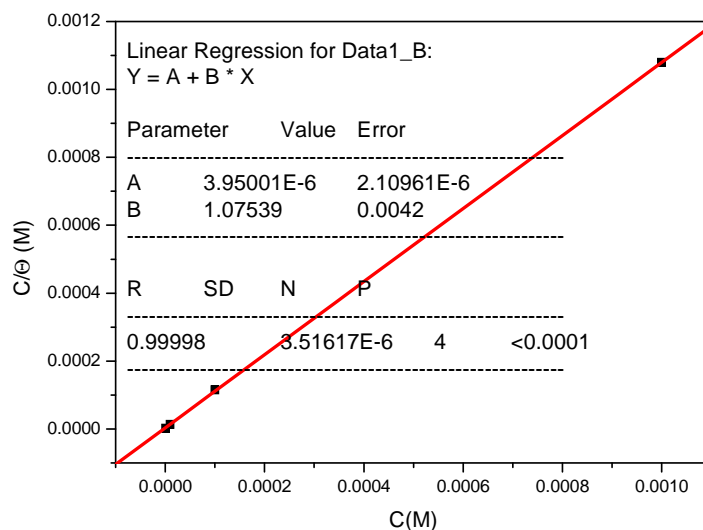


Figure 1. Langmuir adsorption isotherm of synthesized P1 on mild steel in 1 M HCl

Table 2: Parameters of the linear regression between  $C/\theta$  and  $C$  and thermodynamic values of adsorption P1 on the steel mild in 1M HCl media

Inhibitor	Linear correlation	Slope	K	$\Delta G_{ads}^{\circ}$ (kJ mol <sup>-1</sup> )
AE <sub>1</sub>	0.999	1.075	$2.53 \cdot 10^3$	-42.12

The free energy of adsorption  $\Delta G_{ads}^{\circ}$  negative values show a spontaneous process, according to the reference, if the  $\Delta G_{ads}^{\circ}$  value is up to -20 kJ/mol, it is consistent with a physisorption; and those around -40 kJ/mol or higher are consistent with chemisorptions. Our results reveal some values in the average of -40 kJ/mol, which means that the adsorption of P1 on the mild steel is chemisorption [38].

### 3.2. Polarization curves

Anodic and cathodic polarization curves for mild steel in 1M HCl with and without various concentrations of used inhibitor is shown in Figure 2. Various corrosion parameters such as corrosion potential ( $E_{corr}$ ), corrosion current density ( $I_{corr}$ ) and the inhibition efficiency ( $E_p\%$ ) were determined by Tafel extrapolation method and are given in Table 3.

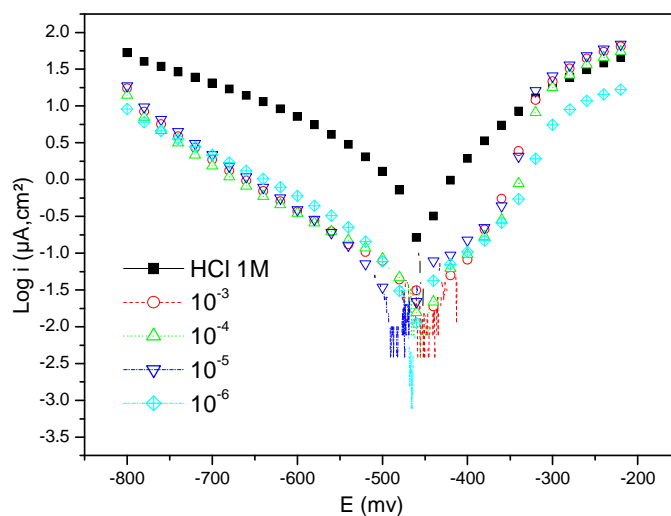


Figure 2. Potentiodynamic polarization curves for mild steel in 1 M HCl without and with various concentrations of the inhibitor (P1)

It is seen that the addition of inhibitor P1 affects the polarisation curves and consequently decreases  $I_{corr}$  significantly for all the studied concentrations, due to increase in the blocked fraction of the electrode surface by adsorption. The cathodic current versus potential curves gave rise to Tafel lines indicating that the hydrogen evolution reaction is activation-controlled,  $\beta_c$  values is quietly modified and then the addition of inhibitor P1 modifies the mechanism of the proton discharge reaction.

In the anodic domain, the presence of P1 hugely decreases anodic current density, the highest effect is observed with P3 and corresponding  $E_p$  attains 94% at  $10^{-3}M$ .

Table 3. Tafel parameters for mild steel corrosion in 1 M HCl without and with various concentrations of the inhibitor (P1)

Inhibitor	Concentration (M)	$-E_{corr}$ (mV/SCE)	$I_{corr}$ ( $\mu A/cm^2$ )	$-\beta_c$ (mV/dec)	$E_p$ (%)
1 M HCl	--	465	1386	184	--
Inhibitor (P1)	$10^{-6}$	455	676	149	51
	$10^{-5}$	454	518	203	63
	$10^{-4}$	458	123	164	91
	$10^{-3}$	456	83	176	94

From these results we can conclude that the corrosion densities calculated by Tafel extrapolation decreased with increasing of inhibitor concentrations. This behaviour reflects that the P1 is adsorbed on the anodic sites and hence inhibition occurs. This means the inhibitor under investigation acts as a mixed type inhibitor. The corrosion potential of the inhibitor containing solution remains almost unchanged to that in the solution without the inhibitor. The slopes of the Tafel line decreases indicating that the inhibition effect is caused by adsorbed inhibiting species [39-40].

### 3.3. Electrochemical impedance spectroscopic studies

Figure 3 presents the Nyquist diagrams obtained in the absence and presence of P1 at different concentrations. The impedance parameters calculated are given in Table 4. The charge-transfer resistance values ( $R_t$ ) were calculated from the difference in impedance at lower and higher frequencies as suggested by Tsuru *et al.* [41].

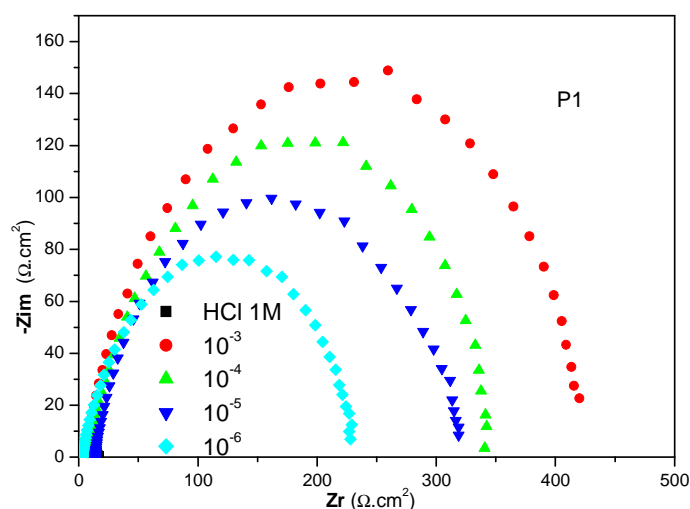


Figure 3. Nyquist plots for mild steel in 1 M HCl containing different concentrations of (P1)

Results obtained show that  $R_t$  increases and  $C_{dl}$  tends to decrease when the concentration of inhibitor increases. A decrease in the  $C_{dl}$  values, which can result from a decrease in the local dielectric constant and/or an increase in the thickness of the electrical double layer, suggests that the P1 function by adsorption at the metal solution/interface [42, 43].

Table 4. AC impedance data of mild steel in 1.0 M HCl acid solution containing different concentrations of (P1) at 308K

Inhibitor	Concentration (M)	$R_t$ ( $\Omega.cm^2$ )	Cdl ( $\mu f/cm^2$ )	$E_{Rt}$ (%)
1 M HCl	--	14.7	200	--
Inhibitor P1	$10^{-3}$	405	76	94
	$10^{-4}$	330	87	93
	$10^{-5}$	300	93	92
	$10^{-6}$	220	103	87

From Table 4, it was clear that charge transfer resistance  $R_t$  values were increased and the capacitance values Cdl decreased with increasing inhibitor P1 concentration. The decrease in the capacitance which can result from a decrease in local dielectric constant and/or an increase in the thickness of the electrical double layer, suggests that the inhibitor molecules act by adsorption at the metal/solution interface.

The results obtained from EIS measurements are in good agreement with that obtained from potentiodynamic polarization and weight loss measurements.

### 3.4. Quantum chemical study

The FMOs (HOMO and LUMO) are very important for describing chemical reactivity. The HOMO containing electrons, represents the ability ( $E_{HOMO}$ ) to donate an electron, whereas, LUMO haven't not electrons, as an electron acceptor represents the ability ( $E_{LUMO}$ ) to obtain an electron. The energy gap between HOMO and LUMO determines the kinetic stability, chemical reactivity, optical polarizability and chemical hardness–softness of a compound [44].

Firstly, in this study, we calculated the HOMO and LUMO orbital energies by using B3LYP method with 6-31G(d,p). All other calculations were performed using the results with some assumptions. The higher values of  $E_{HOMO}$  indicate an increase for the electron donor and this means a better inhibitory activity with increasing adsorption of the inhibitor on a metal surface, whereas  $E_{LUMO}$  indicates the ability to accept electron of the molecule. The adsorption ability of the inhibitor to the metal surface increases with increasing of  $E_{HOMO}$  and decreasing of  $E_{LUMO}$ . The HOMO and LUMO orbital energies and image of **P1** were performed and were shown in Table 5 and Figure 4.

High ionization energy (IE = 7.09 eV) indicates high stability. The number of electrons transferred ( $\Delta N$ ) was also calculated and tabulated in Table 5. The  $\Delta N < 3.6$  indicates the tendency of a molecule to donate electrons to the metal surface [45-46].

Table 5. Quantum chemical descriptors of the studied inhibitor at B3LYP/6-31G(d,p)in gas, G and aqueous, A phases

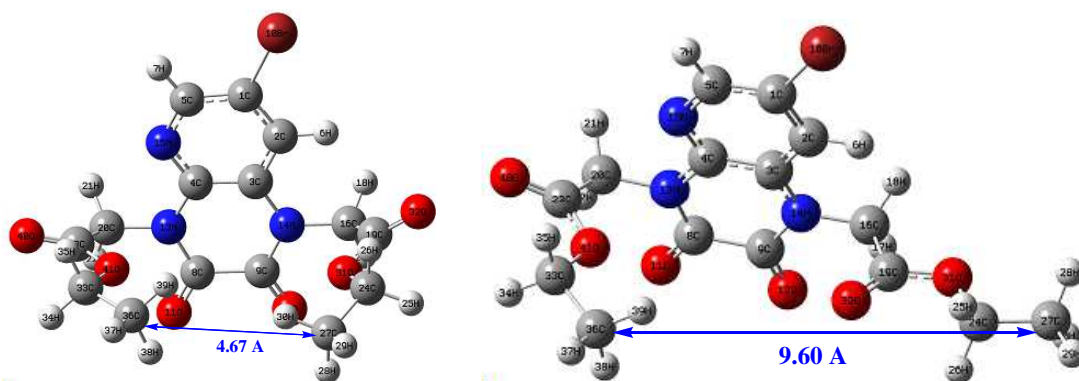
Parameters	Phase	
	Gas	Aqueous
Total Energy $TE$ (eV)	-102543,9	-102544,5
$E_{HOMO}$ (eV)	-7,0923	-4,1327
$E_{LUMO}$ (eV)	-0,6949	-1,9357
Gap $\Delta E$ (eV)	6,3973	2,1969
Dipole moment $\mu$ (Debye)	3,9510	8,2929
Ionisation potential $I$ (eV)	7,0923	4,1327
Electron affinity $A$	0,6949	1,9357
Electronegativity $\chi$	3,8936	3,0342
Hardness $\eta$	3,1987	1,0985
Electrophilicity index $\omega$	2,3697	4,1904
Softness $\sigma$	0,3126	0,9103
Fractions of electron transferred $\Delta N$	0,4855	1,8051

The calculated values of the  $f_k^+$  for all inhibitors are mostly localized on the pyridopyrazine ring. Namely C<sub>2</sub>, C<sub>8</sub>, C<sub>9</sub>, O<sub>11</sub>, O<sub>12</sub> and N<sub>15</sub>, indicating that the pyridopyrazine ring will probably be the favorite site for nucleophilic attacks [47-48].

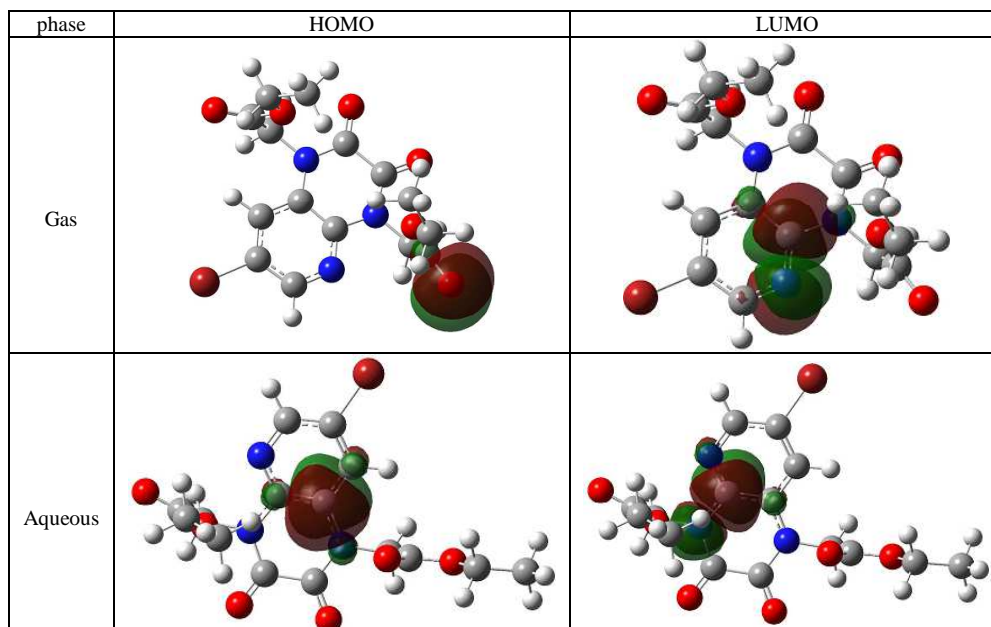
The results also show that O<sub>11</sub> and O<sub>12</sub> atoms are suitable sites to undergo both nucleophilic and electrophilic attacks, probably allowing them to adsorb easily and strongly on the mild steel surface.

**Table 6. Pertinent natural populations and Fukui functions of the studied inhibitors calculated at B3LYP/6-31G(d,p) in gas, G and aqueous, A phases**

Atom <i>k</i>	Phase	$P(N)$	$P(N+1)$	$P(N-1)$	$f_k^+$	$f_k^-$	$f_k^0$
C <sub>2</sub>	G	6,2542	6,3797	6,2385	0,1256	0,0157	0,0706
	A	6,2455	6,3494	6,2334	0,1039	0,0121	0,0580
C <sub>8</sub>	G	5,3839	5,4718	5,3809	0,0879	0,0030	0,0455
	A	5,3762	5,4891	5,3597	0,1129	0,0165	0,0647
C <sub>9</sub>	G	5,3816	5,4721	5,3828	0,0905	-0,0012	0,0446
	A	5,3776	5,4899	5,3617	0,1124	0,0159	0,0641
O <sub>11</sub>	G	8,5502	8,6590	8,4409	0,1088	0,1094	0,1091
	A	8,5898	8,7139	8,4900	0,1241	0,0998	0,1119
O <sub>12</sub>	G	8,5517	8,6594	8,4586	0,1077	0,0931	0,1004
	A	8,5909	8,7137	8,5011	0,1229	0,0898	0,1063
N <sub>15</sub>	G	7,4666	7,5666	7,4557	0,1000	0,0109	0,0555
	A	7,4845	7,5612	7,4624	0,0767	0,0221	0,0494

**Figure 4. Optimized molecular structures of the studied inhibitor calculated in gas and aqueous phases at B3LYP/6-31G(d,p) level of P1**

After the analysis of the theoretical results, we can say that the acetate groups are farthest in aqueous phase ( $C_{36}-C_{37}=9.60 \text{ \AA}$ ) than as the gas phase ( $C_{36}-C_{37}=4.67 \text{ \AA}$ )

**Table 7. The HOMO and the LUMO electrons density distributions of the studied inhibitors computed at B3LYP/6-31G (d,p) level in gas and aqueous phases**

## CONCLUSION

On the basis of these results, the following conclusions may be drawn:

- P1 inhibit the corrosion of mild steel in 1M HCl.
- The inhibition efficiency increases with increasing of inhibitor concentration to attain a maximum value of 94 % at 10<sup>-3</sup> M.
- Polarisation study shows that P1 act as mixed-type inhibitor.
- In determining the corrosion, electrochemical studies and weight loss measurements give similar results.
- The calculated quantum chemical parameters such as HOMO-LUMO gap, E<sub>HOMO</sub>, E<sub>LUMO</sub>, dipole moment ( $\mu$ ) and total energy (TE) were found to give reasonably good correlation with the efficiency of the corrosion inhibition.
- We can also say that the acetate group distances are hisgher in aqueous phase than gas phase.

## REFERENCES

- [1] R.Cavier, *Chim. Ther.* **1966**, 66, 327-330.
- [2] T. J.Haley, A. M. Flesher; R.Vcomelt, *Proc. Soc. Biol. Med.* **1957**, 96, 579-584.
- [3] G.Cavallini, E.Massarani, D.Nardi, F.Magrassi, P.Altucci, *J. Med. Pharm. Chem.* **1959**, 1, 327-332.
- [4] J. Carroll Temple, J. D. Rose , R. D. Elliott , J. A. Montgomery ,*J. Med. Chem.* **1968**, 11 (6),1216–1218.
- [6] B.Mathew, S. Srivastava, *Bioorganic & Medicinal Chemistry*, **2011**, 19, 7120-7128.
- [5] F.Wiseloge, In: Armarego WLF,editor. *Advances in hetero cyclic chemistry*, New York: *Academic Press*, **1963**, 1, 304.
- [7] B.David J. (avid J. Blythin, North Caldwell; Ho-Jane Shue, Pine Brook, both of NJ)... *U.S Patent Documents*: 4760073, **1988**.
- [8] shimazaki , norihiko, nagakuni, tsuchiura-shi, ibaraki, SAWADA, akihiko, WATANABE, shinya, PCT/JP 96/03666 ; patent WO97/24355, **1997**.
- [9] E. E. Ebenso, N. O. Eddy and A. O. Odiongenyi, *Portugaliae Electrochimica. Acta*, **2009**, 27(1), 13.
- [10] N.O. Eddy and S.A. Odoemelum , *Adv. Nat. & Appl. Sci*, **2008** ,2(1) ,35.
- [11] I.B. Obot, N. O. Obi-Egbedi, S.A. Umoren, *Int. J. Electrochem. Sci*, **2009**, 4, 863.
- [12] E.E. Ebenso, H. Alemu, S.A. Umoren, I.B.Obot, *Int. J. Electrochem. Sci*, **2008**, 3, 1325.
- [13] S.A. Umoren, I.B. Obot, E.E. Ebenso, N. O. Obi-Egbedi, *Int. J. Electrochem. Sci*, **2008**, 3, 1029.
- [14] I.Cherif Alaoui, Y. Kandri Rodi, E.M.El Hadrami, A. Haoudi, M. Skalli, B. Garrigues and E.M. Essassi, *J. Mar. Chim. Heterocyclic*, **2007**, 6 (1), 32-37.
- [15] M.J.Frisch,G.W.Trucks,H.B.Schlegetal., Gaussian 09, Revision A.1, Gaussian, Inc.,*Wallingford, Conn, USA*, **2009**.
- [16] H. Elmsellem, M. H.Youssouf, A. Aouniti, T. Ben Hadd, A. Chetouani, B. Hammouti. *Russian, Journal of Applied Chemistry*, **2014**, 87(6), 744–753.
- [17] J. Li, H. Li, M. Jakobsson, S. Li, P. Sjodin, M. Lascoux, *Mol. Ecol.* 21, 28 (2012)[4] K. Yamamoto, T. Irimura, *J. Biochem*, **2011**, 150, 477.
- [18] H. Elmsellem, A. Aouniti, M. Khoutou, A. Chetouani, B. Hammouti, N. Benchat, R. Touzani and M. Elazzouzi, *J. Chem. Pharm. Res*, **2014**, 6, 1216.
- [19] H. Elmsellema, T. Haritb, A. Aouniti, F. Malekb, A. Riahi, A. Chetouani, and B. Hammouti, *Protection of Metals and Physical Chemistry of Surfaces*, **2015**, 51(5), 873–884.
- [20] K. Efil and Y. Bekdemir, *Canadian Chemical Transactions*, **2015**, 3(1), 85.
- [21] L. Pauling, *The nature of the chemical bond*, 3rd edn. (Cornell University Press, Ithaca, **1960**).
- [22] K.D. Sen, C. Jorgenson, Springer. Berlin, **1987**, 66.
- [23] K.D. Sen, D.M.P. Mingos, Springer, Berlin, **1993**, 80.
- [24] R.G. Parr, W. Yang, Oxford University Press, Oxford, **1989**.
- [25] P. Geerlings, F. de Proft, W. Langenaeker, *Chem. Rev*, **2003**,103, 1793.
- [26] H. Chermette, *J. Comput. Chem*, **1999**, 20, 129.
- [27] R.G. Parr, R.A. Donnelly, M. Levy, W. Palke, *J. Chem. Phys*, **1978**, 68, 3801.
- [28] P. Hohenberg, Kohn, *Phys. Rev. B*, **1964**, 136, 864.
- [29] W. Kohn, L. Sham, *J. Phys. Rev. A*, **1965**, 140, 1133.
- [30] R.G. Parr, R.G. Pearson, *J. Am. Chem. Soc*, **1983**, 105, 7512.
- [31] W. Yang, W. Mortier, *J. Am. Chem. Soc*, **1986**, 108, 5708.
- [32] R.K. Roy, S. Pal, K. Hirao, *J. Chem. Phys*, **1999**, 110, 8236.
- [33] R.G. Pearson, *Inorg. Chem.*, **1988**, 27, 734.
- [34] V.S. Sastri, and Perumareddi, J.R., *Corrosion*, **1997**, 53, 671
- [35] P. Udhayakala, T. V. Rajendiran, and S. Gunasekaran, *Journal of Chemical, Biological and Physical Sciences A*, **2012**, 2(3), 1151-1165.
- [36] H. Elmsellem, A. Aouniti,M. Khoutou, A. Chetouani, B. Hammouti, N. Benchat, R. Touzani and M. Elazzouzi, *J. Chem. Pharm. Res*, **2014**, 6, 1216.
- [37] N. K. Sebbar, H. Elmsellem, M. Boudalia, S. lahmidi, A. Belleaouchou , A. Guenbour, E. M. Essassi, H. Steli, A. Aouniti, *J. Mater. Environ. Sci*, **2015**, 6 (11), 3034-3044.

- [38] H. Elmsellem, A. Elyoussfi, H. Steli, N. K. Sebbar, E. M. Essassi, M. Dahmani, Y. El Ouadi, A. Aouniti, B. El Mahi, B. Hammouti, *Der Pharma Chemica*, **2016**, 8(1), 248-256.
- [39] A. Aouniti, H. Elmsellem, S. Tighadouini, M. Elazzouzi, S. Radi, A. Chetouani, B. Hammouti, A. Zarrouk, *Journal of Taibah University for Science*, **2015**, <http://dx.doi.org/10.1016/j.jtusci>.
- [40] H. Elmsellem, K. Karrouchi, A. Aouniti, B. Hammouti, S. Radi, J. Taoufik, M. Ansar, M. Dahmani, H. Steli and B. El Mahi, *Der Pharma Chemica*, **2015**, 7(10), 237-245.
- [41] T. Tsuru, S. Haruyama, B. Gijutsu, *J. Jpn. Soc. Corros. Eng.* **1978**, 27, 573.
- [42] H. Elmsellem, H. Nacer, F. Halaimia, A. Aouniti, I. Lakehal, A. Chetouani, S. S. Al-Deyab, I. Warad, R. Touzani, B. Hammouti. *Int. J. Electrochem. Sci*, **2014**, 9, 5328.
- [43] H. Elmsellem, N. Basbas, A. Chetouani, A. Aouniti, S. Radi, M. Messali, B. Hammouti, *Portugaliae. Electrochimica. Acta*, **2014**, 2, 77.
- [44] M. Govindarajan, M. Karabacak, *Spectrochim Acta Part A Mol Biomol Spectrosc*, **2012**, 85, 251-60.
- [45] N.K. Sebbar, H. Elmsellem, M. Boudalia, S. Iahmidi, A. Belleaouchou, A. Guenbour, E. M. Essassi, H. Steli, A. Aouniti, *J. Mater. Environ. Sci*, **2015**, 6(11), 3034-3044
- [46] H. Elmsellem, A. Elyoussfi, N.K. Sebbar, A. Dafali, K. Cherrak, H. Steli, E.M. Essassi, A. Aouniti, B. Hammouti, *Maghreb. J. Pure & Appl. Sci*, **2015**, 1, 1-10.
- [47] I. Lukovits, E. Kalman, F. Zucchi, *Corrosion*, **2001**, 57, 3-7.
- [48] K. F. Khaled, *Applied Surface Science*, **2010**, 256(22), 6753-6763.